A R C H I V E S O F M E T A L L U R G Y A N D M A T E R I A L S
Volume 54 2009 Issue 1

K. NALEPKA*, P. NALEPKA**

ANALYSIS OF QUANTUM EFFICIENCY OF THIN FILM SOLAR CELL BASED ON FORMULATED ADDITIVE MODEL

ANALIZA KWANTOWEJ SPRAWNOŚCI FOTO-OGNIW CIENKOWARSTWOWYCH OPARTA NA SFORMUŁOWANYM ADDYTYWNYM MODELU

The aim of the paper is to formulate an additive model enabling more effective optimization of silicon solar cells. According to the model, a flux of carriers flowing through the one dimensional, simple p-n junction is divided into components connected with processes occurring in the cell i.e. generation, front surface recombination, back surface recombination, respectively. Each of the component fluxes is defined by an appropriate quantum efficiency subsequently subjected an analysis. The introduced component quantum efficiencies become new optimization criteria. The separate consideration of the processes makes easier to formulate design criteria for solar cells. The obtained results open the possibility to study solar cells, in which the light trapping methods are applied, e.g. texturization.

Celem pracy jest sformułowanie addytywnego modelu umożliwiającego efektywniejszą optymalizację foto - ogniw krzemowych. Zgodnie z modelem strumień nośników przepływający przez jednowymiarowe, proste złącze p-n podzielono na składniki związane z procesami zachodzącymi w foto - ogniwie, czyli odpowiednio z: generacją, rekombinacją na powierzchni przedniej, rekombinacją na powierzchni tylnej. Każdy strumień składowy został zdefiniowany przez odpowiednią kwantową sprawność poddaną następnie analizie. Wprowadzone składowe kwantowe sprawności stają się nowymi kryteriami optymalizacyjnymi, których suma stanowi kwantową sprawność foto – ogniwa. Odrębne rozpatrywanie każdego z procesów w znacznym stopniu upraszcza formułowanie kryteriów projektowych. Otrzymane wyniki otwierają możliwość studiowania foto - ogniw, w których zastosowano metody pułapkowania światła np. teksturyzację.

1. Introduction

Quantum efficiency (QE) reflects the cell design and the material quality [1], [2]. Analysing QE when device parameters undergo changes we can increase solar cell efficiency. With regard to a large number of the parameters the study requires to apply a computer program for example PC-1D [3] or/ and complex analytical models. In the paper, quantum efficiency was presented in a form of sum of components connected with processes proceeding in the solar cell, that is generation and recombinations. Then the role of the particular processes in the device performance results from comparison of quantum efficiencies assigned to them but not from the magnitude of parameters crucial for them [4]. Thus, as it was shown in the paper, the participation of back surface recombination can be reduced not only by decrease in effective surface recombination rate, but also by choice of an appropriate generation profile. The introduced division of solar cell quantum efficiency allows considering each of the processes separately. Thus, we can limit a number of parameters analysed together. At the same time, with regard to less complex physical situation, determination of optimal relations between them becomes easier.

An additive model formulated in the paper was based on R.J. Schwartz and J.L Gray conception [5]. They illustrated operation of the solar cell by a funnel that had holes of different shapes and size in it. Let's consider a stationary flow of liquid when the funnel is filled up to a fixed level. A stream, poured into the top of the funnel, flows out not only through the bottom, but also through the side holes. The first outflow represents a carrier flux delivered by the solar cell (J_{SC}), whereas the side leakages correspond to the recombination of minority carriers (J_{rec}).

Described analogy was an inspiration to build a model, in which the flux J_{SC} was resolved into three

* CRACOW UNIVERSITY OF TECHNOLOGY, INSTITUTE OF STRUCTURAL MECHANICS, 31-155 KRAKÓW, 24 WARSZAWSKA STR., POLAND
** AGRICULTURE UNIVERSITY OF CRACOW, DEPARTMENT OF ENGINEERING AND MACHINERY FOR FOOD INDUSTRY, 131-149 KRAKÓW, 22 BALICKA STR., POLAND

contributions connected with processes of generation or recombination, respectively. The model enables to observe the solar cell operation in various, exterior conditions. Thanks to this we can formulate design criteria for achieving high efficiency solar cells.

2. Model

The basic element of the model is p-n junction bounded by external planes. It was formed by acceptor and donor, uniform doping. Concentrations of the impurities amounted to N_D and N_A, respectively. The doping caused arising of dopant ions and majority carriers, which distributions were shown in Fig.1.

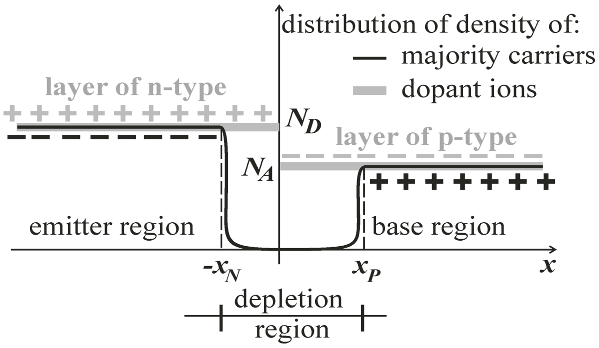

Fig. 1. Distributions of density of the dopant ions and the majority carriers in the simple p-n junction, which is in the equilibrium state

As a result, we obtained the quasi-neutral regions (the base and the emitter) and the space – charge region (the depletion region) contained between coordinates: $-x_N$, x_P [6] Apart from the majority carriers, there are also present the minority carriers. In the base wafer we have electrons characterized by the diffusion coefficient D_n and in the emitter wafer – holes of the diffusion coefficient D_p. When the p-n junction is in the equilibrium state, the minority carriers concentration is constant in the particular wafers and amounts to n_i^2/N_A in the case of electrons, n_i^2/N_D in the case of holes, where n_i is the intrinsic carriers concentration [6]. Data applied in the calculations are presented in Tab.1.

TABLE

Metallic radii of rare earth metals and magnesium [12]

Parameter	Value
N_A	$1 \cdot 10^{16}$ cm^{-3}
N_D	$1 \cdot 10^{19}$ cm^{-3}
x_N	$9.4 \cdot 10^{-5}$ μm
x_P	$9407 \cdot 10^{-5}$ μm
D_p	2 cm^2/s
D_n	40 cm^2/s

The model describes operation of the formed p-n junction when the processes of: generation, recombination at the front surface and recombination at the rear surface are introduced in sequence. In particular, the model was used to analyse changes in the thin film solar cell efficiency induced by widening of the layers of n and p type (Fig.1).

3. Generation

The formed p-n junction was unbalanced by monochromatic exposure of the front surface. As a result, in the solar cell, there appeared carriers forming a generation flux (Fig.2).

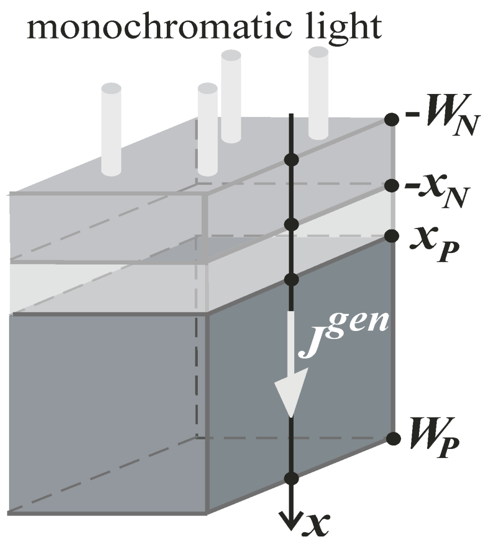

Fig. 2. Scheme showing arising of the generation flux in the solar cell

If density of the generation flux – $J^{gen}(E)$ will be referred to density of the photon flux falling on the front surface – $b_s(E)$, we obtain a generation quantum efficiency $QE^{gen}(E)$. Let's assume, that rate of the generation is expressed by the following formula:

$$G(x, E) = b_s(E)\alpha(E)e^{-\alpha(E)\cdot(W_N+x)} \tag{1}$$

where $\alpha(E)$ is the absorption coefficient for photons of energy E.

Then $J^{gen}(E) = \int_{-W_N}^{W_p} G(x, E)dx$, and the generation quantum efficiency takes the form:

$$QE^{gen}(E) = 1 - e^{-\alpha(E)\cdot(W_N+W_P)} \tag{2}$$

$QE^{gen}(E)$ determines the probability, with which an incident photon of energy E will deliver one electron to the external circuit at the absence of any recombination processes. The magnitude of the generation quantum efficiency depends on thickness of n and p type layers.

Let's take into consideration a thin film solar cell, in which W_N = 0.25μm and W_P = 50μm. With regard to small thickness of the n-type layer, its widening, even several times, induces negligible increase in QE^{gen}. Different result is obtained in case of widening of the p-type layer. Let's assume, that W_P takes the value typical for currently manufactured solar cells i.e. 300 μm. Then, in the range of infrared, the generation quantum efficiency increases significantly, but when radiation energy rises, the generation process intensifies and moves towards the front surface, what causes smaller and smaller increase in QE^{gen}. Consequently for α=1000 $^1/_{\text{cm}}$ QE^{gen} amounts to 0.2%, merely (Fig.3). Accordingly, we can say, that, in the range of visible radiation, increase in the generation quantum efficiency induced by widening of the p-type layer from 50μm to 300μm is relatively small.

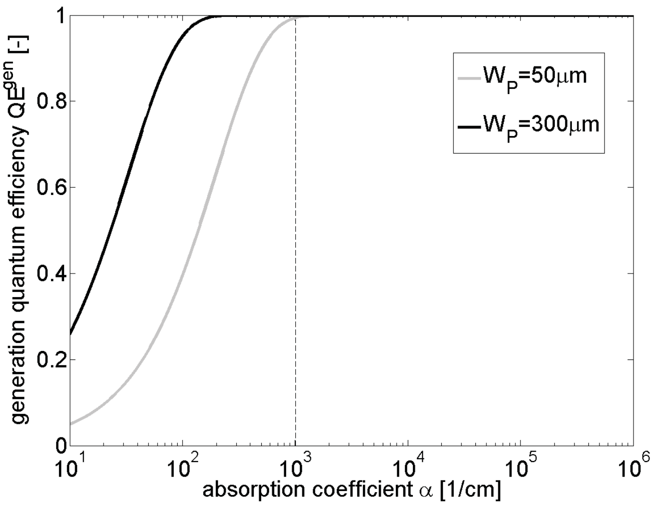

Fig. 3. Generation quantum efficiency QE^{gen} in dependence on the absorption coefficient α for the p-type layer of the various thickness

Density of the generation flux $J^{gen}(E)$ is constant through the device. However, in dependence on considered point x, there is different participation of hole and electron carriers in the flux. These first moving in the direction of the x-axis form a hole generation flux of the density: $J_p^{gen}(E,x) = \int_{-W_N}^{x} G(E,x\prime)dx\prime$, whereas these second displacing opposite to the x-axis form an electron generation flux of the density: $J_n^{gen}(E,x) = \int_{W_P}^{x} G(E,x\prime)dx\prime$ (fig.4).

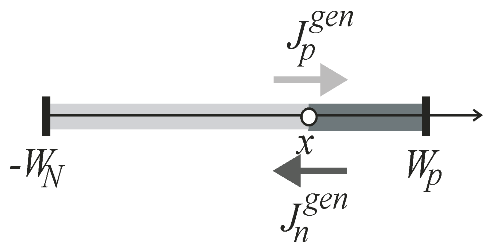

Fig. 4. Scheme showing arising of the hole and electron generation fluxes (J_p^{gen}, J_n^{gen}), which are components of the generation flux (J^{gen})

The distinguished fluxes can be characterized by appropriate quantum efficiencies:

$$QE_p^{gen}(E,x) = 1 - e^{-\alpha(E)\cdot(W_N+x)}, \quad QE_n^{gen}(E,x) = e^{-\alpha(E)\cdot(W_N+W_p)} - e^{-\alpha(E)\cdot(W_N+x)} \tag{3}$$

where: $QE_p^{gen}(x,E) - QE_n^{gen}(x,E) = QE^{gen}(E)$
Absolute values of the quantum efficiencies | $QE_p^{gen}(x,E)$ |, | $QE_n^{gen}(x,E)$ | are probabilities with which an incident photon of energy E introduces, in the point x, one carrier belonging to the hole or electron generation flux, respectively. The sign of the quantum efficiency determines the direction of the carriers' motion. The distinguished hole and electron generation fluxes are related with the excess concentrations of minority carriers by the appropriate diffusion laws:

$$J_p^{gen}(x) = -D_p \frac{d\Delta p_N^{gen}(x)}{dx}, \quad J_n^{gen}(x) = -D_n \frac{d\Delta n_P^{gen}(x)}{dx} \tag{4a 4b}$$

Of course, there should be fulfilled a continuity equation, which in the of case hole carriers takes the following form:

$$\frac{dJ_p^{gen}(x)}{dx} = G(x) \tag{5}$$

Additionally, if the flow of hole carriers is induced only by the generation process, then at the front surface of the solar cell $J_p^{gen}(-W_N) = 0$. Besides we assume that the externally applied voltage V_{ext}=0. Then, the concentrations of the minority carriers at the surfaces bounding the depletion region take the equilibrium values, so $\Delta p_N^{gen}(-x_N) = 0$, $\Delta n_p^{gen}(-x_N) = 0$. To sum up, there were determined the conditions, which allow to evaluate the generation excess hole concentration occurring at the front surface $\Delta p_N^{gen}(-W_N)$. For rate of the generation expressed by the formula (1) we get:

$$\Delta p_N^{gen}(-W_N) = -\frac{1}{D_p} \int_{-x_N}^{-W_N} \int_{-W_N}^{x} G(x\prime)dx\prime dx = \frac{b_S}{D_P\alpha}[e^{-\alpha(W_N-x_N)} + \alpha(W_N - x_N) - 1] \tag{6}$$

Analogically, we can evaluate the generation excess electron concentration occurring at the rear surface:

$$\Delta n_P^{gen}(W_P) = -\frac{1}{D_n}\int_{-x_P}^{W_P}\int_{-W_P}^{x} G(x\prime)dx\prime dx = \frac{b_S}{D_n\alpha}[e^{-\alpha(x_P+w_N)} - (1+\alpha(W_P-x_P))e^{-\alpha(W_P+W_N)} \qquad (7)$$

The introduced quantities: $\Delta p_N^{gen}(-W_N)$ and $\Delta n_P^{gen}(W_P)$ are essential for the recombination process considered later. Let's analyse how their magnitude changes when the front surface is exposed to monochromatic radiation of various wavelengths. At first, in the range of infrared, the increase in the radiation energy induces increase in the excess hole concentration at the front surface as well as the excess electron concentration at the rear surface. However, the further increase in the absorption coefficient causes cumulation of more and more quickly proceeding generation near the front surface. Accordingly, $\Delta p_N^{gen}(-W_N)$ still increases, while $\Delta n_P^{gen}(W_P)$ gradually decreases along with decaying of the generation process in the base region. The magnitude of the excess minority carriers concentration at the external surfaces depends on the thickness of the emitter and the base region (Fig.5,6).

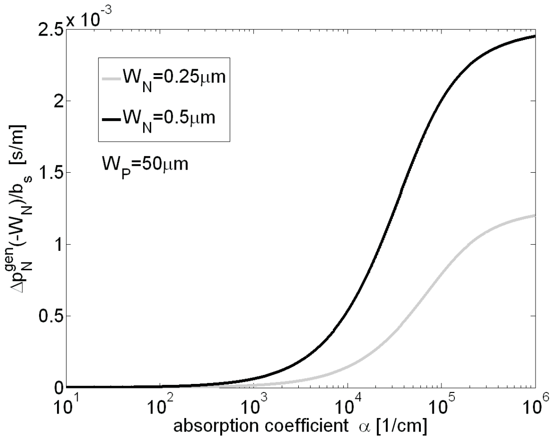

Fig. 5. Excess hole concentration at the front surface induced by the photon flux of unitary density $\Delta p^{gen}(-W_N)/b_s$ as a function of the absorption coefficient at the thicknesses of the *n* and *p* layer amounting to W_N and W_P=50μm respectively

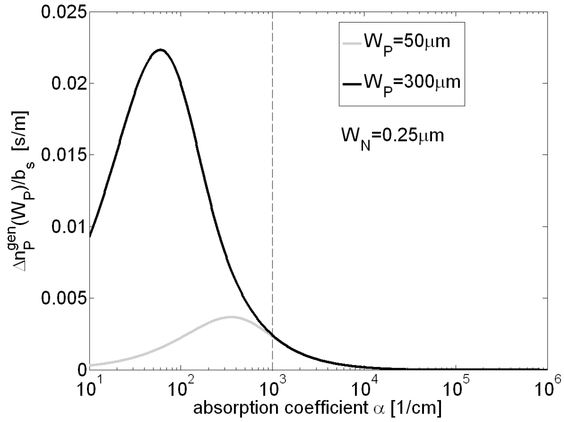

Fig. 6. Excess electron concentration at the rear surface induced by the photon flux of unitary density $\Delta n^{gen}(W_P)/b_s$ as a function of the absorption coefficient at the thicknesses of the *n* and *p* layer amounting to W_N=0.25μm and W_P respectively

Widening of the n type layer causes appearance of two additional hole fluxes in the increment region: $\Delta W_N = W_N' - W_N$. The first of them is constant since the carriers arising in the original emitter form it. The second one, by contrast, is generated in the increment region. The presence of these additional fluxes causes the increase in the excess hole concentration of a constant value in the whole original emitter region. The magnitude of the increment can be evaluated by usage of the diffusion law (4a). Thus widening of the emitter region induces increase in the excess hole concentration at the front surface (Fig.5) expressed as follows:

$$\Delta p_N^{gen}(W_N', E) - \Delta p_N^{gen}(W_N, E) = \frac{-1}{D_P}\int_{x_N}^{(x_N+\Delta W_N)}\int_{-W_N}^{x} G(x\prime, E)dx\prime dx \qquad (8)$$

The analogical analyse can be carried out in the case of widening of the p type layer. This time, however, occurs the increase in the excess electron concentration at the rear surface. The reason is an additional electron flux, which appears in the whole base region. The carriers generated in the base increment: $\Delta W_P = W_P' - W_P$ and then moving towards the depletion region form the flux. Their concentration at the rear surface is the increment of $\Delta n_P^{gen}(W_P)$ resulting from widening of the p type layer. Thus, according to the diffusion law, we get:

$$\Delta n_P^{gen}(W_P', E) - \Delta n_P^{gen}(W_P, E) = \frac{-1}{D_N}\left[\int_{W_P}^{W_P+\Delta W_P}\int_{W_P+\Delta W_P}^{x} G(x\prime, E)dx\prime dx + (W_P - x_P)\int_{W_P+\Delta W_P}^{W_P} G(x, E)dx\right. \qquad (9)$$

Of course the increment of the excess electron concentration at the rear surface induced by the base widening depends on the radiation energy. If the absorption coefficient is sufficiently large then the generation rate in the base increment becomes evanescent. Thus, considering lack of the additional flux, the excess electron concentration at the rear surface doesn't change despite the base widening. If we take the earlier analysed solar cell then such a case will occur already in the range of visible radiation when $\alpha > 1000^{1}/_{\mathrm{cm}}$. (fig.6)

4. Recombination

The presence of the unsaturated bonds at the external surfaces induces recombination in these regions. The rate of the recombination is proportional to the excess concentration of the minority carriers at the external surfaces: $\Delta p_N(-W_N)$ and $\Delta n_P(W_P)$, respectively [6], [7]. As a result, two surface recombination fluxes arise: hole and electron. The first of them is directed opposite and the second according to the x – axis (Fig.7). Their densities $J_P^{R,SF}$, $J_n^{R,SF}$ equal to the surface recombination rates. Thus we get:

$$J_P^{R,SF} = -S_{F.eff}\Delta p_N(-W_N), \quad J_n^{R,SF} = S_{BSF}\Delta n_P(W_P) \qquad (10a\ 10b)$$

where $S_{F.eff}$, S_{BSF} are the effective recombination rates at the front and back surface, respectively.

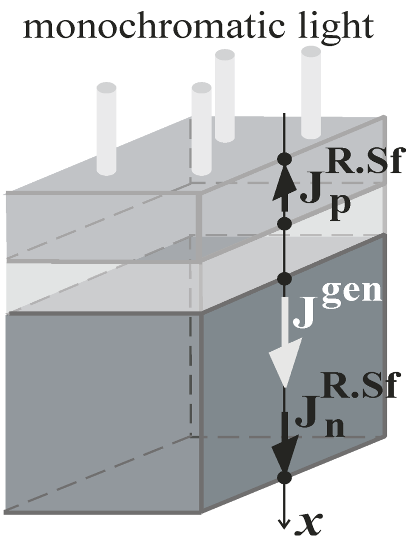

Fig. 7. Scheme showing decomposition of the total flux of the carriers moving through the solar cell into three constituents: J^{gen}, $J_p^{R.Sf}$, $J_n^{R.Sf}$. They are related to the processes of: generation, hole recombination at the front surface, electron recombination at the rear surface

Using the continuity equation (5), the diffusion law (4a) for the total hole flux $J_P(x)$ and simultaneously allowing for the conditions in the form: (10a), $\Delta p_N(-x_N) = 0$ we can determine the distribution of the excess hole concentration in the n-type layer: $\Delta p_N(x)$. The linearity of the differential operator enables to write $\Delta p_N(x)$ in the form of two summands:

$$\Delta p_N(x) = \Delta p_N^{gen}(x) + \Delta p_N^{R,SF}(x) \qquad (11)$$

The first of them is related to the occurring generation and the second to the surface recombination. Usage of the introduced decomposition enables us to write the density of the hole flux of the surface recombination in the form:

$$J_P^{R,Sf}(E) = \frac{-S_{F.eff}D_P}{D_P + S_{F.eff}(W_N - x_N)}\Delta p_N^{gen}(E,-W_N) \qquad (12)$$

So $J_P^{R,SF}$ is proportional to the generation excess hole concentration at the front surface: $\Delta p_N^{gen}(E,-W_N)$ given by the expression (6). The similar relation was obtained for the electron flux of the surface recombination:

$$J_n^{R,SF}(E) = \frac{S_{BSF}D_n}{D_n + S_{BSF}(W_P - x_P)}\Delta n_P^{gen}(E,W_P) \qquad (13)$$

where $\Delta n_P^{gen}(E,W_P)$ is given by the formula (7).

The expressions (12), (13) show that the dependence of the densities of the recombination fluxes: $J_P^{R,SF}(E)$, $J_n^{R,SF}(E)$ on the radiation energy represented by the changing absorption coefficient α is as in the case of the generation excess concentrations: $\Delta p_N^{gen}(E,-W_N)$ and $\Delta n_P^{gen}(E,W_P)$, respectively (Fig.5,6).

If we refer $J_P^{R,SF}$ and $J_n^{R,SF}$ to the density of the photon flux: b_s then we will get the quantum efficiencies for the carriers belonging to the hole and electron flux of the surface recombination: $QE_P^{R.SF}$ and $QE_n^{R.SF}$. Similarly as in the case of the generation, the absolute values: $|\ QE_P^{R.SF}\ |$and $|\ QE_n^{R.SF}\ |$ can be interpreted as the probabilities. This time however, they concern arising of the carriers belonging to the recombination fluxes. The signs of the quantum efficiencies: $J_P^{R,SF}$ and $J_n^{R,SF}$ result from the movement direction. So in the case of the hole we get the negative value and in the case of the electron the positive value. The magnitudes of the quantum efficiencies: $J_P^{R,SF}$ and $J_n^{R,SF}$ depend on the thickness of the n and p – type layers, respectively. Widening of the emitter layer induces increase in both generation part and the recombination one of the excess hole concentration at the front surface. The increment of the positive $\Delta p_N^{gen}(E,-W_N)$ is greater then increment of the negative $\Delta p_N^{R.SF}(E,-W_N)$, independently from the radiation energy and the effective recombination rate $S_{F.ef}$, what can be proved mathematically. The reason is the high rate, with which the generation process occurs in the emitter layer.

To sum up, widening of the n-type layer induces increase of the quantum efficiency for the carriers belonging to the hole recombination flux, that is disadvantageous effect. The similar analysis can be carried out in the case of the p – type layer. This time, however, widening can bring about the advantageous effect in the form of decrease in the quantum efficiency: | $QE_n^{R.SF}$ |. Let's take into consideration the monochromatic radiation of the energy sufficiently large to induce the cumulation of the generation process near the front surface. In that case, widening of the base layer causes negligibly small increase in the generation excess electron concentration at the rear surface, as it was shown in the chapter 3. However, there occurs increase in | $\Delta n_P^{R.SF}(W_P)$ |, so we obtain decrease in the quantum efficiency: | $QE_n^{R.SF}$ |. Such a case we can observe in the range of visible radiation, when $\alpha > 1000^1/_{\mathrm{cm}}$ (Fig.8a, 8b). When the radiation energy begins to decrease then widening of the base layer will induce not only increase in the recombination part, but also the generation one of the excess electron concentration at the rear surface. If the increment of $\Delta n_P^{gen}(W_P, E)$ exceeds the increment | $\Delta n_P^{R.SF}(W_P, E)$ |, the quantum efficiency | $QE_n^{R.SF}$ | will increase. In the case of the earlier considered solar cell, this situation arises when $\alpha < 198^1/_{\mathrm{cm}}$ and $S_{BSF} = 10^{4\mathrm{cm}}/\mathrm{s}$ (fig. 8a, 8b).

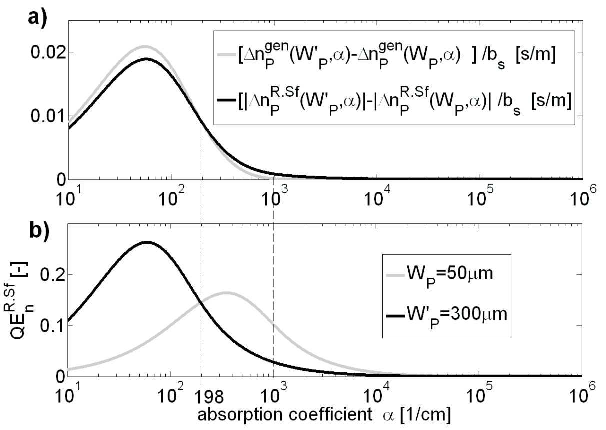

Fig. 8. a) Increments of the absolute values of two components of the excess electron concentration at the rear surface as functions of the absorption coefficient α. The increments were referred to the density of the photon flux b_s to eliminate its influence. The first component $\Delta n_P^{gen}(W_P, \alpha)$ is connected with the generation process and the second one $\Delta n_P^{R.SF}(W_P, \alpha)$ with back surface recombination process. The widening of the base layer from W_P = 50μm to W_P' = 300μm causes the increments of the particular constituents. The calculations were carried out for $S_{BSF} = 10^{4\mathrm{cm}}/\mathrm{s}$. b) The quantum efficiency for the carriers belonging to the electron flux of the surface recombination $QE_n^{R.SF}$ as a function of the absorption coefficient α. The dependence was considered for two thicknesses of the p-layer: W_P = 50μm, W_P' = 300μm and $S_{BSF} = 10^{4\mathrm{cm}}/\mathrm{s}$. The relation between $QE_n^{R.SF}(W_P, \alpha)$ and $QE_n^{R.SF}(W_P', \alpha)$ results from the course of the curves showed in Fig. 8a

The generation and the surface recombination, which are crucial for designing of effective thin solar cells [8] were considered. Beside these processes, there occurs also the bulk recombination. Allowance for it induces the change in the excess concentration of the minority carriers at the external surfaces and consequently the change in the surface recombination fluxes. The rate of the recombination of the holes in the n – type layer is negligibly small because the diffusion length L_p exceeds the thickness W_N several times. As a result, we can assume that $QE_P^{R.SF}$ remains unchanged. In the case of the thin devices, the decrement of $QE_n^{R.SF}$ is also small. It was showed in Fig.9.

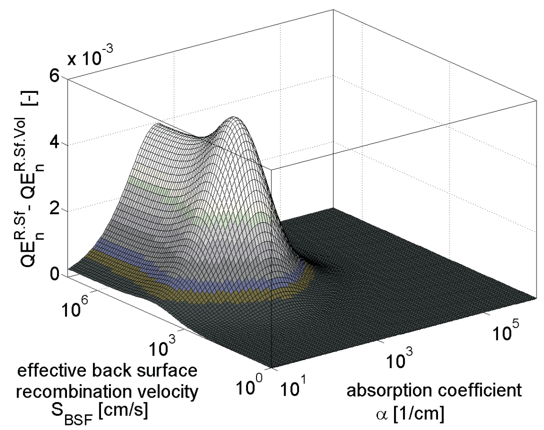

Fig. 9. Difference of two quantum efficiencies for carriers belonging to the electron flux of surface recombination as a function of the absorption coefficient and effective back surface recombination velocity S_{BSF}. In the case of the first of them $QE_n^{R.SF}$, electron bulk recombination is disregarded. On the contrary, the second one $QE_n^{R.Sf.Vol}$ allows for it. The electron diffusion length L_n = 140μm was assumed

Description of the processes occurring in thin solar cells is the main task of the carried out analysis. Therefore the bulk recombination was disregarded. This assumption was kept during the analysis of changes in the quantum efficiencies induced by widening of the emitter and base layers.

5. Conclusions

According to the created model, the total flux of the carriers moving through the solar cell was resolved into three components related to the occurring processes. Thus, the solar cell quantum efficiency can be written in an analogical form:

$$QE(E) = QE^{gen}(E) + QE_P^{R.Sf}(E) - QE_n^{R.Sf}(E). \quad (14)$$

The particular components are related to the processes of: generation, hole recombination at the front surface and electron recombination at the back surface, respectively. The negative sign was ascribed to the third summand because the solar cell quantum efficiency QE, was defined in the base of the hole flux. The presence of the two last addends, taking negative values, lowers QE, what is very well illustrated by the funnel analogy described earlier.

Similarly to the solar cell quantum efficiency, its change induced by widening of the emitter or base layer can be written in the additive form. If we increase W_N, then the change in the generation quantum efficiency and the quantum efficiency for carriers belonging to the electron flux of surface recombination can be disregarded, what was explained earlier. On the contrary, we get the increment of the quantum efficiency for carriers belonging to the hole flux of surface recombination $\Delta QE_P^{R.Sf}(E)$. In the rage of high-energy radiation $\Delta QE_P^{R.Sf}(E)$ can take substantial values. Thus, widening of the emitter layer leads to reduction of the quantum efficiency (QE). In the case of the considered solar cell the decrement of QE can achieve 15%, what is illustrated in Fig.10.

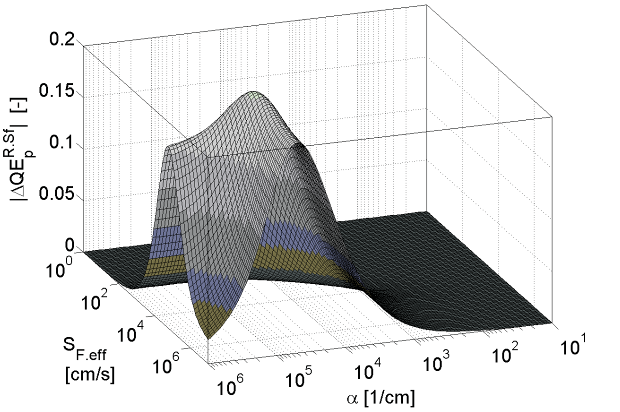

Fig. 10. Increment of quantum efficiency for carriers belonging to hole flux of surface recombination | $\Delta QE_P^{R.Sf}$ | as a function of the absorption coefficient and effective front surface velocity $S_{F.eff}$. The increment is induced by the widening of the n-type layer from W_N = 0.25μm to W'_N = 0.5μm at the p-type layer thickness W_P = 50μm

Widening of the base layer causes the change in two summands: the generation quantum efficiency and the quantum efficiency for carriers belonging to the electron flux of surface recombination. If effective back surface recombination velocity is low then the second component will remain unaltered. Thus $\Delta QE^{gen}(E)$ will determine the change in the solar cell quantum efficiency. In the case of the considered solar cell, this situation arises for $S_{BSF} < 10^2$ cm/s (Fig.11). Accordingly, Fig.12 for $S_{BSF} < 10^2$ cm/s shows the dependence of the increment of the generation quantum efficiency on radiation energy. When recombination velocity S_{BSF} takes values typical for solar cells, widening of the base layer induces, beside $\Delta QE^{gen}(E)$, the change in the quantum efficiency for carriers belonging to the electron flux $\Delta QE_n^{R.Sf}(E)$. Dependence of $\Delta QE_n^{R.Sf}(E)$ for various values of the effective back surface recombination velocity was presented in Fig.11. In the low energy, infrared radiation, generation process occurs very intensively near the rear surface. Therefore, according to the previous considerations, widening of the base layer leads to the increment of $QE_n^{R.Sf}$. Fig 11 shows that $\Delta QE_n^{R.Sf}$ can exceed 20%. In the range of visible radiation we get decrement of $QE_n^{R.Sf}$, independently from the magnitude of the effective recombination velocity S_{BSF}. According to the Fig.11 $\Delta QE_n^{R.Sf}$ can achieve -20%. Overall, the base widening induces increase in the solar cell quantum efficiency. In the infrared, the reason is increment of the generation quantum efficiency, to some degrees, reduced by increment of $QE_n^{R.Sf}$. On the contrary, in the range of visible radiation increase in QE results mainly from decrement of the recombination quantum efficiency $QE_n^{R.Sf}$. The higher the effective recombination velocity S_{BSF} the larger | $\Delta QE_n^{R.Sf}$ | (Fig.11). If in the led considerations we allowed for the bulk recombination, then described increase in the solar cell quantum efficiency would be kept, but at the same time there would appear an additional decrease. The reason of the obtained decrement would be increase in the bulk recombination velocity $\Delta R(x)$ induced by widening of the base layer.

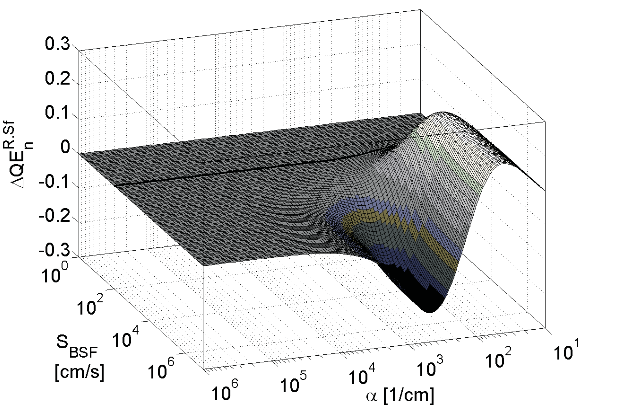

Fig. 11. Change in the quantum efficiency for carriers belonging to electron flux of surface recombination $\Delta QE_n^{R.Sf}$ as a function of the absorption coefficient and effective back surface velocity S_{BSF}. The increment is induced by the widening of the p-type layer from W_P = 50μm to W'_P = 300μm at the n-type layer thickness W_N = 0.25μm

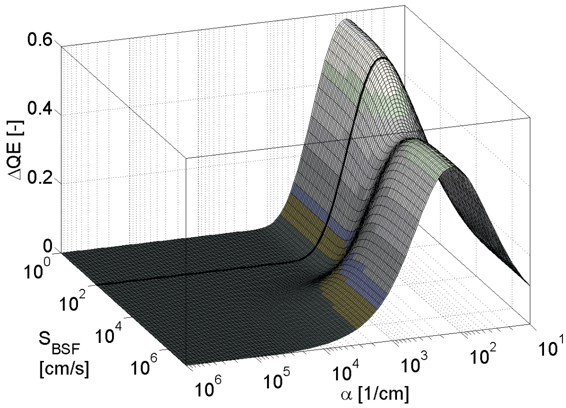

Fig. 12. Increment of the quantum efficiency ΔQE as a function of the absorption coefficient α and the effective back surface velocity S_{BSF}. The increment is induced by the widening of the p-type layer from W_P = 50μm to W'_P = 300μm at the n-type layer thickness W_N = 0.25μm

The presented additive model shows participation of the particular components in increase in the solar cell quantum efficiency. Increment of the generation quantum efficiency and decrement of the recombination one can be obtained without the change in the base thickness. In this aim, light trapping methods are applied. Then, through the change in the generation profile, the increase in QE^{gen} is obtained [9], [10], [11]. The formula (13) derived in chapter 4 shows that the second component: $QE_n^{R.Sf}$ can be decreased not only by reducing S_{BSF}, but also by lowering of the generation excess concentration of electrons at the back surface: $\Delta n_p^{gen}(W_P)$. Thus, appropriately formed the generation profile enables additional enhancement of solar cell quantum efficiency.

Received: 10 May 2008.

Acknowledgements

This work was supported by the Polish State Committee for Scientific Research within the frame of the Project PBZ/100/T08/2003.

REFERENCES

[1] P. A. B a s o r e, IEEE Trans. On Electron Devices **ED-37**, 337-343 (1990).
[2] P. K i t t i d a c h a c h a n et al., Sol. Energy Mater. Sol. Cells **91**, 160-166 (2007).
[3] P. B a s o r e, D. C l u g s o n, PC-1D version 4 for windows: from analysis to design, in: Proceedings of the 25th IEEE Photovoltaic Specialist Conference, Washington, 337-381 USA, 1996.
[4] P. A. B a s o r e, Extended spectral analysis of internal quantum efficiency, in: Proceedings of the 23rd IEEE Photovoltaic Specialist Conference, Louisville, 147-152 USA, 1993.
[5] J. L. G r a y, The Physics of the Solar Cell in: A. Luque, S. Hegedus ed., Handbook of Photovoltaic Science and Engineering John Wiley & Sons, 61-112 (2003).
[6] M. S. T y a g i, Introduction to semiconductor materials and devices, John Wiley & Sons (1991).
[7] J. N e l s o n, The Physics of the Solar Cells, Imperial Collage Press (2003).
[8] F. L l o p i s, I. T o b i a s, Sol. Energy Mater. Sol. Cells **87**, 481-492 (2005).
[9] A. M a h d j o u b, L. Z i g h e d, Thin Solid Films **478**, 229-304 (2005).
[10] M. Y. G h a n n a m, IEEE Trans. On Electron Devices **ED-46**, 2072-2079 (1999). bibitem11 A l - O m a r, M. Y. G h a n n a m, Sol. Energy Mater. Sol. Cells **52**, 107-124 (1998).